MODELING AND CORRECTING SPATIAL NON-UNIFORMITY OF THE APEX PUSHBROOM IMAGING SPECTROMETER

Daniel Schläpfer, Johannes W. Kaiser, Jens Nieke, Jason Brazile, and Klaus I. Itten
University of Zurich, Switzerland [a]

1 INTRODUCTION

The Airborne Prism Experiment (APEX) is currently being built as a demonstrator and calibrator for potential future European spaceborne imaging spectrometers (Itten et al., 1997, Schaepman et al., 2003). It allows the retrieval of traditional and new products for vegetation, geological, limnological and atmospheric sciences. The uniformity of pushbroom imaging spectrometers is affected by spectral and spatial misregistration within each detector array as well as by coregistration errors between the VNIR and the SWIR spectral range (Mouroulis et al., 2000). Correction of such persistent effects may only be done by dedicated interpolation methods. However, any interpolation produces spectra which may differ from real uniform measurements. The impact of interpolation techniques on the uniformity is tested by evaluating their impact on the radiometric measurements. It has to be evaluated, which correction strategies can increase the overall uniformity of the system while maintaining the radiometric accuracy. An extensive library of measured surface reflectance spectra as well as samples of AVIRIS imaging spectrometer data are used for these analyses. The original spectra are systematically convolved to distorted positions, wherefrom correction methods are applied to retrieve the original values. The radiometric residual error can be quantified taking the expected APEX pixel misregistration error into account in the sensor model. Potential improvements can then be modeled by interpolations to uniform positions.

For correction of such effects, a scheme has to be defined. Such a scheme is given for correction of these effects in the data calibration chain of the APEX system. It uses straightforward coordinate transformation methods to correct for higher order distortions, as they have to be expected in a real pushbroom instrument. The results have to be weighted against the radiometric accuracy requirements of the system as defined in Schläpfer and Schaepman (2002).

1.1 The APEX Instrument in Comparison to AVIRIS

APEX, being a pushbroom type imaging spectrometer with two 2-dimensional detectors, i.e. CCD and CMOS, is designed fundamentally differently than AVIRIS (Green et al., 1998). However, it covers almost the same spectral range as AVIRIS does, and basically has very similar performance numbers (see Table 1). Thus, AVIRIS data are a useful testbed for all kinds of radiometric analysis required for evaluation and testing of the APEX processing and archiving facility (PAF) development.

[a] *Department of Geography, RSL, University of Zürich, Winterthurerstr. 190, CH-8057 Zürich, Switzerland, Phone: +41 1 635 52 50, Fax: +41 1 635 68 46, E-mail: dschlapf@geo.unizh.ch*

Table 1: Comparison of APEX and AVIRIS performance.

Parameter	APEX	AVIRIS
Field of View (FOV)	± 14° deg	± 17.2° deg
Instantaneous Field of View (IFOV)	0.48 mrad	0.99 mrad
Flight altitude	2'000 m.a.g. - 12'000 m.a.s.l.	3'000 m.a.g.- 20'000 m.a.s.l.
Across track pixels	1000	677
Scan frequency	20 – 40 Hz	12 Hz
Spectral bands	VNIR: 312 (114 programmable binned) SWIR: approx. 199	224
Spectral range	380 – 2500 nm	(370-) / 410-2510 nm
Spectral sampling interval	380– 870 nm: < 5 nm, 870 – 2500 nm: < 10 nm	10 nm
Imaging principle	Pushbroom Prism Spectrometer	Whiskbroom Grating Spectrometer
Storage capacity on board (online / offline)	> 300 GByte	35 GB/Tape
Dynamic Range	14 bit	12 bit
Positional knowledge	0.2 pixels	~ 1 pixel
Stabilization	Stabilized platform to ±5% of FOV	none

1.2 Selected Data Sets

Nine exemplary data sets have been selected as a test bed for the presented analysis (see Figure 2). They include various surface types from city and agricultural areas to geological sites and desert. Eight of the nine data sets have been recorded between 1998 and 2001 while one data set from 1995 has been added for evaluation of the influence of SNR on the results. For 1998-2001, the AVIRIS system is assumed to be stable. Furthermore, the spatial resolution varies between 3 and 20 meters as both high and low altitude data were included.

The second data set engaged is an artificial test data set. A spectral data cube has been derived from the SPECCHIO spectral database (Bojinski et al., 2003). The database includes a wide representative range of more than 4000 natural and simulated surface reflectance spectra. The data has been modeled to at-sensor radiance data using the MODTRAN4 radiative transfer code (Berk et al., 1998). The spatial distribution of the spectra is done on a regular grid of 3x3 and optionally 5x5 pixels. This result was ordered in a complete spectral data cube at 1-2 nm spectral resolution (see Figure 1).

Figure 1: Spectral database based artificial image, in a (partially) thematically ordered spatial structure. Each visible patch of image pixels represents one spectrum of the database.

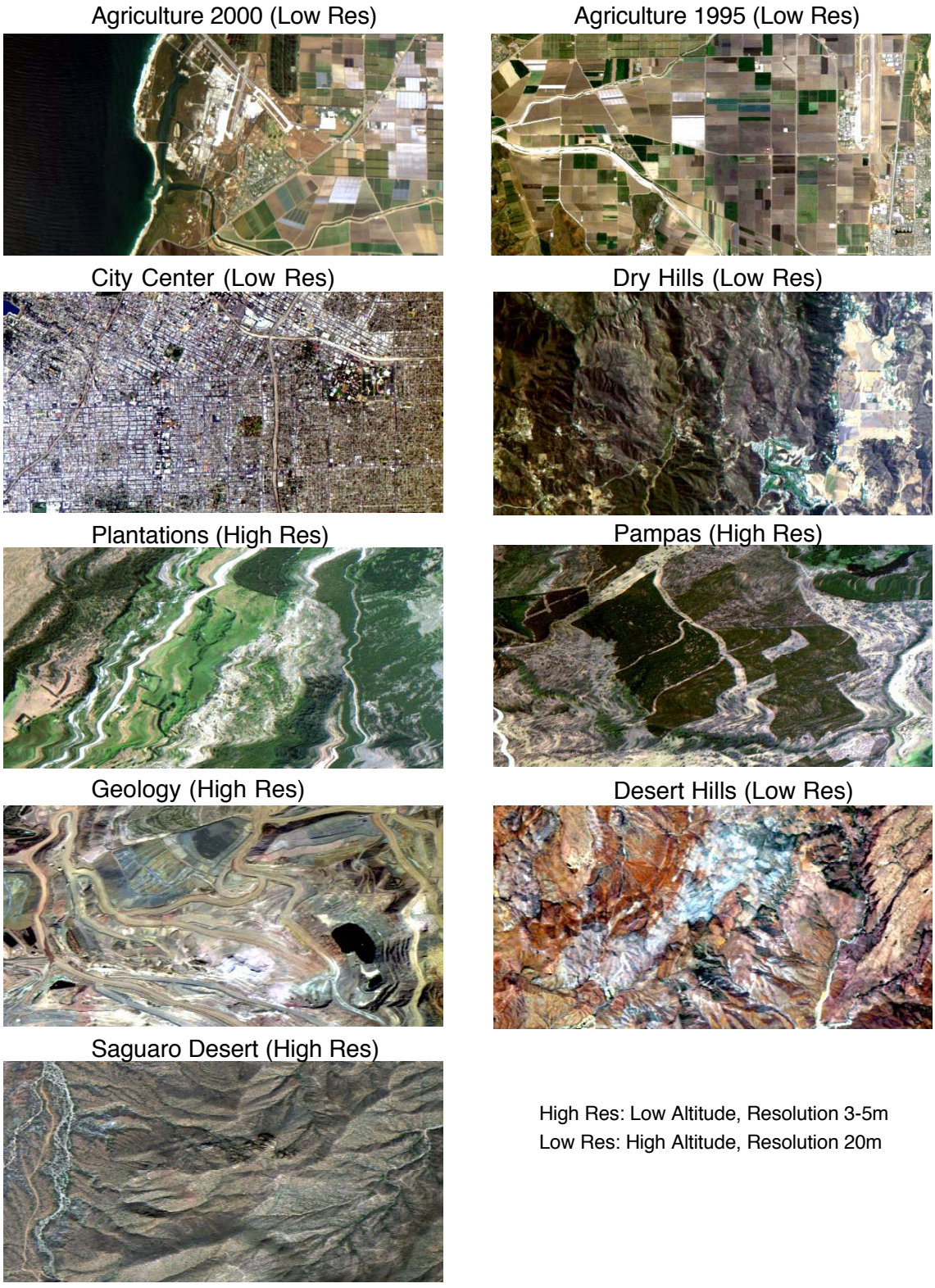

Figure 2: AVIRIS test data sets used for PSF analyses.

2 METHODS

The sensor Point Spread Function (PSF) describes the spatial and spectral response of a sensor (Schowengerdt, 1997). With this work, two PSF effects affecting uniformity of a spectrum in the spatial domain are investigated (i.e., the 'spatial uniformity'). First, the band-to-band variations of the PSF width (at full width half maximum; FWHM) are analyzed and second, the PSF center position difference between the visible (VNIR) and the shortwave infrared optical channel is quantified. The spatial misregistration is analyzed with respect to its impact on radiometric deviations from a perfectly uniform product.

2.1 PSF Width Variation Analysis

The spatial PSF of the APEX system is non-uniform with respect to two dimensions: in the across track direction, PSF width differences of about 5-20% lead to variations of the spatial resolution. Secondly, band-to-band PSF width variations in the range of 3-10% lead to non-uniformity of the acquired spectra.

The currently expected APEX PSF values are used for analysis of the influence of PSF variations on uniformity. Current estimates of the spectral PSF RMS min/max values are depicted in Figure 4 (top) for both dimensions (along and across track); showing the spectral dependency. All test data sets are systematically convolved to the range of PSF characteristics following a procedure depicted in Figure 3. First, the data is convolved using the overall average PSF of the system in both directions across and along track. In a second step, the mean PSF at each wavelength (i.e., spectral band) is calculated and the original data is convolved with these PSF values. The difference between the convolved bands is then taken as a measure of potential deviations due to PSF variations, affecting the spatial uniformity of one pixel spectrum. The standard deviation of the absolute difference is taken in relation to the image mean values to obtain an estimate on the errors, as depicted in Figure 4 for the artificial data.

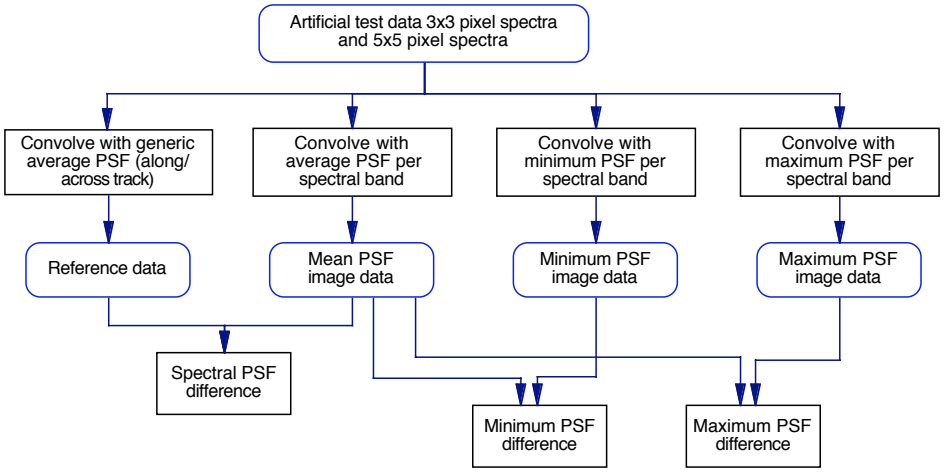

Figure 3: Workflow of the calculations to derive the influence of PSF-width variation.

The same image original is then convolved to the minimum and maximum PSF of each spectral wavelength and compared to the image convolved at mean spectral PSF. Variations in a range of 1-2% are introduced by the spectral and the so modeled spatial non-uniformity of the PSF. The very same calculations have been done on a second artificial data set consisting of 5x5 pixel patches of the same spectrum. Here, the errors are reduced by about 20% but still remain in the 1-2% range. Note, that the spectral and the across track error are treated quasi independently in these results and thus

may be superimposed at each wavelength to obtain an estimate of the expected error due to PSF non-uniformity. However, the spatial non-uniformity of spectra is of much higher relevance than the across track variations since it introduces disliked spectral inconsistencies to the data. Figure 4 depicts the analysis for the most extreme PSF values at each spectral band. The differences increase to as much as 3% for the worst case while the spatial non-uniformity leads to a 1%-level error.

The very same analysis then applied to the AVIRIS test images. A similar spectral behavior can be observed (see Figure 5). An obvious difference is seen between high and low resolution images, which reflects the spatial smoothing of the lower resolution. The 1995 data set of agriculture shows much more discrepancies. This is mainly due to the lower SNR performance before the major refurbishment of the AVIRIS system. It also shows that SNR limits the correction possibilities for spatial non-uniformity.

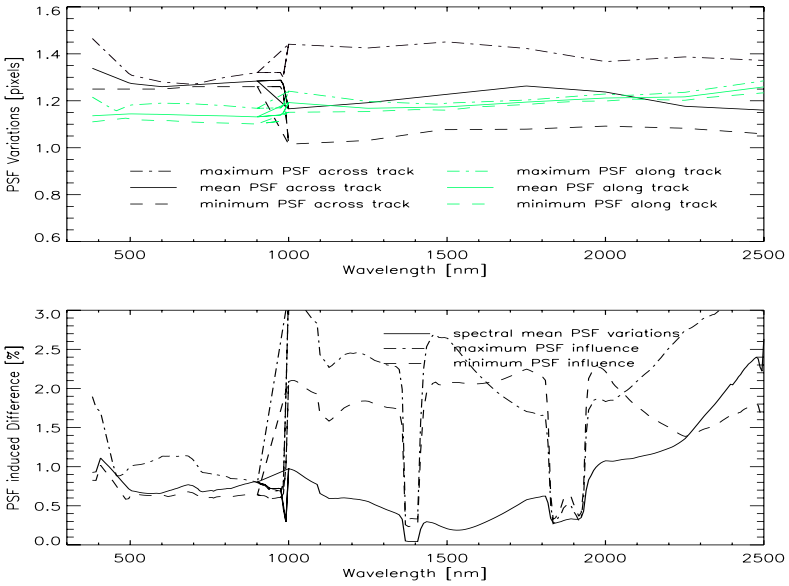

Figure 4: Influence of PSF variations: top: APEX PSF values, bottom: maximum across track variation and mean non-uniformity calculated on 3x3 patches of the artificial spectral database image.

2.2 Co-Registration Analysis

The last issue is the spatial co-registration between the two detectors (i.e., APEX channels). For APEX, a spatial misregistration in a range up to 0.71 pixels is currently expected. This offset is simulated by defining two distinct sensor models, which are then applied in a simulated scan over the artificial image scene. The convolution is done on the simulated at-sensor radiance spectra as described above for both data sets; with the artificial 3x3 patches and with the AVIRIS test data sets, respectively.

The simulated at sensor data is first convolved to the mean along/across track 2D-PSF of the sensor. Registered pixels are then derived from the degraded data by linear interpolation as depicted in Figure 6. First, a sensor model of 1000 across track pixels is put in an 'ideal' straight line on this pattern, covering one pixel along track and 998 pixels across track. Second, the coregistration offset (effective in across track direction only) is added to the sensor model and a second interpolation is performed using this second sensor model. The standard deviation of the difference of these two interpolates is then taken as measure for the coregistration error. A number of 40 image lines is taken

for the 3x3 pixels case. These image lines cover almost the whole spectral database with its broad variety of realistic spectra. For AVIRIS data, 200 lines have been selected covering the subset images, resulting in 200'000 test spectra.

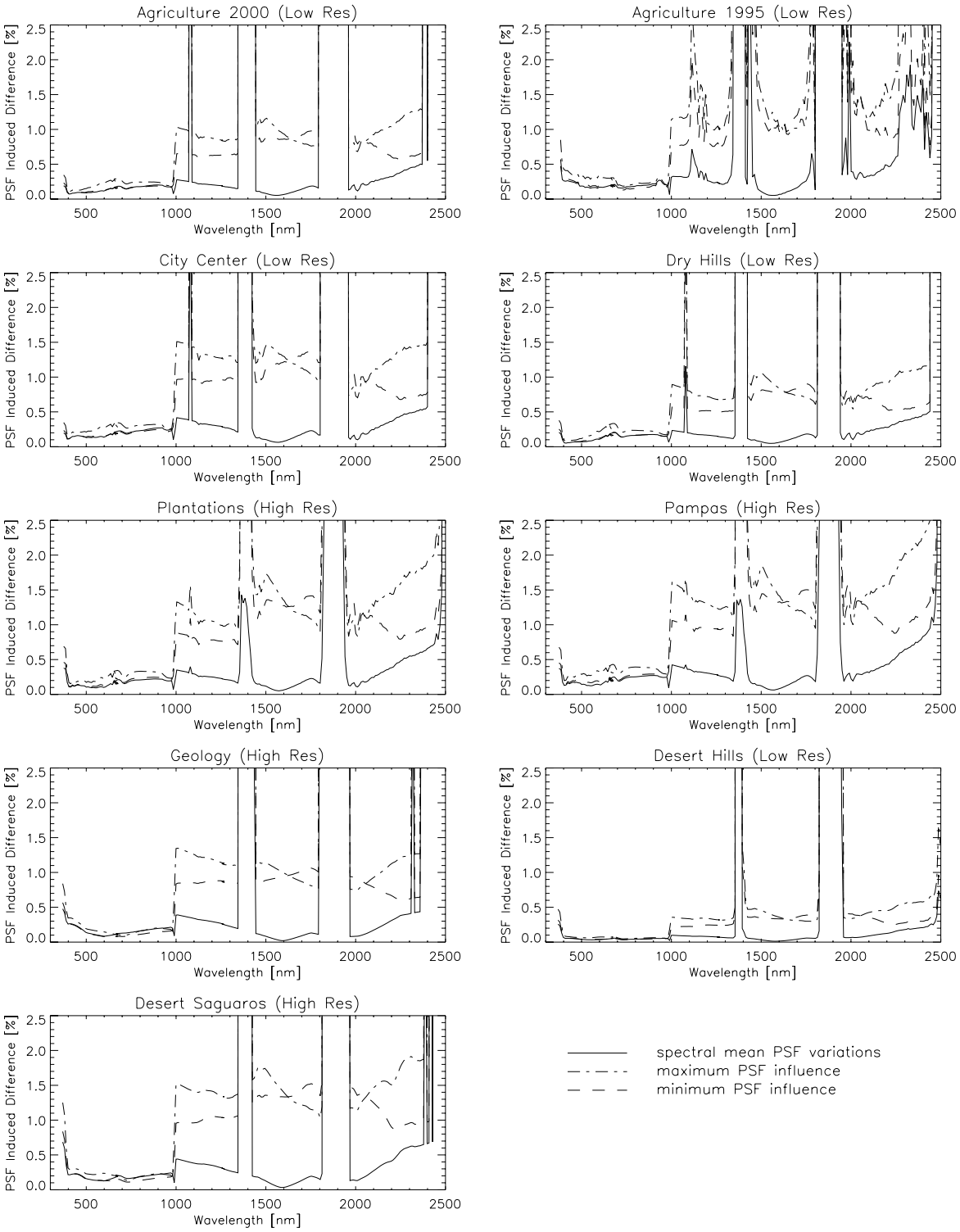

Figure 5: Impact of PSF variations on spatial uniformity as calculated from AVIRIS test image cubes.

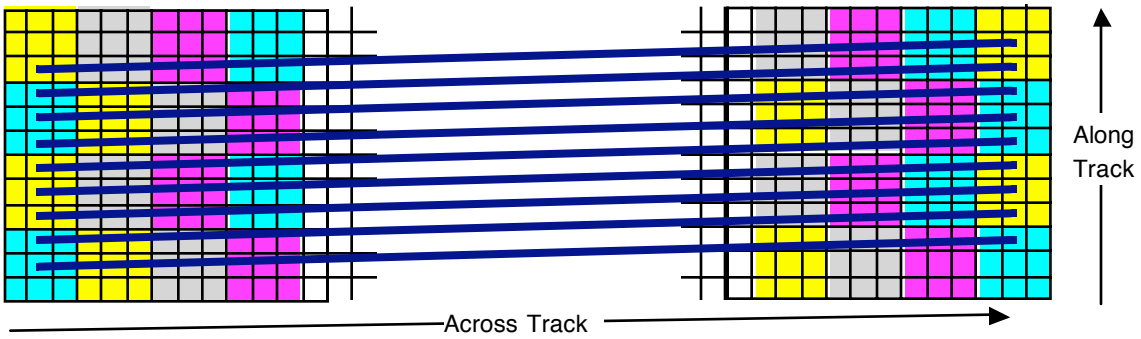

Figure 6: Coregistration analysis scheme on 3x3 pixels artificial data cube. A sensor tilted by one pixel across track and stretched by 2 pixels along track is put on top of the artificial at sensor radiance data. The thick blue lines depict the slightly tilted and stretched across track sensor model consisting of 1000 pixels distributed over the artificial spectral image raster.

The misregistration effect is quantified as standard deviation of the difference between the re-sampled imagery using the ideal and the distorted sensor model. Relative differences of at-sensor radiance reaching more than 10% are observed between the two sensor models for the artificial data (see Figure 7). To improve the situation, across track linear interpolation is applied to the distorted data in order to recover the original image positions. The linear interpolation reduces the error to a level of 2%. This error might be further reduced by using dedicated deconvolution or improved interpolation routines. First attempts using deconvolution or quadratic interpolation routines as implemented in IDL (RSI Inc.) did not lead to significantly improved results. Further investigations would have to be made in order to reduce the error caused by coregistration problems of the APEX system. However, it is not expected that this effect can be fully eliminated by post-processing in the PAF.

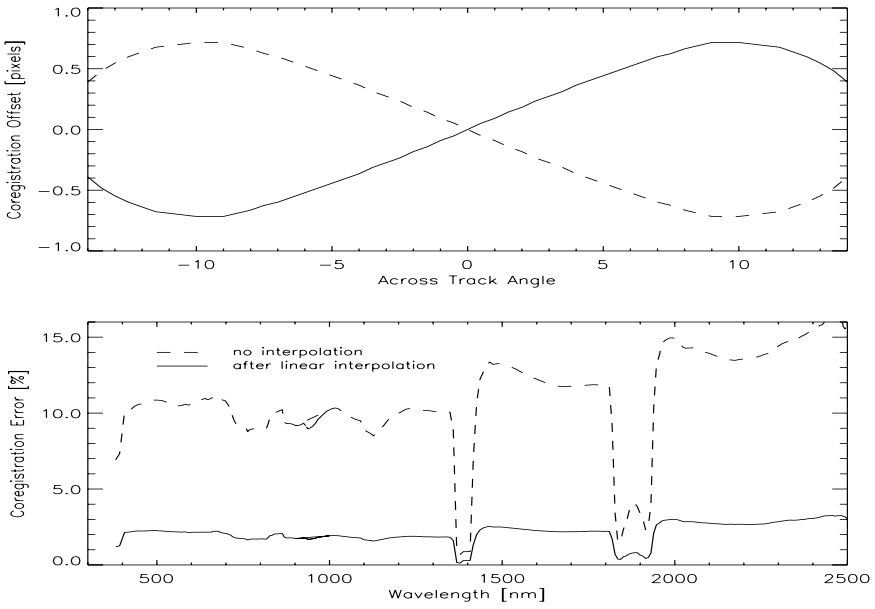

Figure 7: Misregistration error derived from calculations on 3x3 pixels artificial data cube.

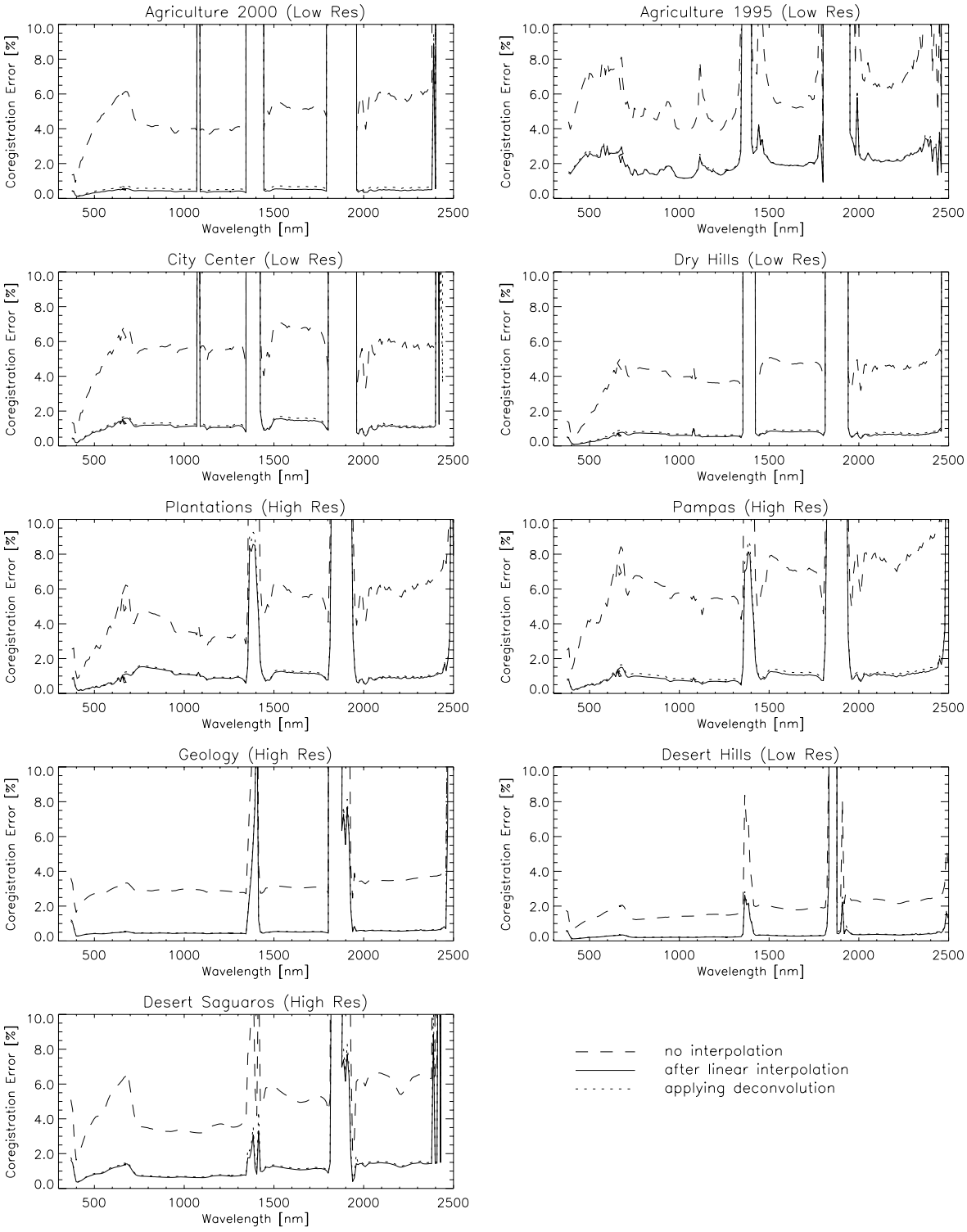

Figure 8 Impact of spatial misregistration on spectral accuracy, before and after linear interpolation, as calculated on AVIRIS test image cubes.

If the misregistration analysis is performed on AVIRIS data, the absolute values are lower than on the artificial data but generally show the same behavior as depicted in Figure 8. Again, much larger and harder to correct influences are observed in 1995 AVIRIS data, while low resolution natural scenes are less sensitive. Due to the spatial nature of Cities, most effects can again be observed on this example scene, even at low resolution.

3 APEX DATA PROCESSING

3.1 Overview

The operational APEX radiance data product will be generated by the Processing and Archiving Facility (PAF) developed at RSL, University of Zurich. The scheme foresees radiometric data calibration as well as an optional step for assuring spatial and spectral uniformity. Since APEX performs freely programmable spectral binning, an initial step of un-binning also needs to be performed. Therefore, the following processing sequence has been established and implemented:

(1) Undo binning
(2) Correct the readout smear effect of the VNIR detector
(3) Correct for dark current
(4) Invert pixel response, i.e. gain function, to physical units
(5) Replace bad pixels
(6) Correct stray light and, optionally, ghost images
(7) Correct, optionally, spectral and spatial non-uniformity
(8) Redo binning

The non-uniformity correction algorithms are detailed below. The other data processing steps are described in Schläpfer et al. (2003). A description of the underlying instrument model and the processing of the required calibration parameters is given in Kaiser et al. (2003).

3.2 Actual Pixel Coordinates

The actual PSFs of a number of selected pixels will be annually characterized along with the other calibration parameters in so-called Calibration Home-Base (CHB) at the DLR, Munich, Germany. Thus the PSF center wavelengths λ and across-track θ angles are obtained for a limited number of pixels. The values for all pixels are modeled with a couple of 2-dimensional polynomials for each of the detectors:

$$\theta_{VNIR/SWIR}(y,z) = b \quad + b_1 z + b_2 y + b_3 z^2 + b_4 y^2 + b_5 zy \,, \tag{2}$$

where y and z are continuous representations of the pixel indices in the two detector dimensions and the sets of coefficients a and b are derived from the pixel characterizations performed in the laboratory. This parameterization requires separate treatment of each detector and un-binned data. After the characterization of the real instrument different parameterizations may be substituted for the polynomials.

3.3 Uniformity

3.3.1 Smile / Frown

The spectral and spatial across-track PSF center position non-uniformity is also called smile/frown effect or spectral line curvature. It is described quantitatively by equations (1, 2). The instrument records data on a uniform *y-z* grid while most applications require data on a uniform λ-θ grid. Thus uniformity is achieved by a transformation of the data from *y-z* to λ-θ coordinates. Technically, this transformation involves the inversion of equations (1, 2) and a resampling of the observed radiances in the wavelength and across-track directions.

The transformation can be employed to obtain the observed radiances to an arbitrary λ-θ grid. The uniformity requirement only demands that the λ values be constant in θ direction and vice versa. The PAF actually chooses the grid such that the errors induced by the re-sampling are minimized by ensuring that the average deviation of from the λ-θ values of the actual detector pixels is minimal. For the smile/frown correction two separate uniform target grids are found for the two detectors. These grids will ultimately be visible in the radiance product as the nominal λ-θ grid(s) of APEX.

3.3.2 PSF Width

The non-uniform smoothing in both spatial directions due to the variation of the PSF's width is not corrected during the processing since it would either degrade the observations unnecessarily or introduce unwanted a priori information during a deconvolution.

3.3.3 Coregistration

The coordinate transformation described above for the smile/frown correction can handle arbitrary target grids. Thus, it is also used to obtain uniform radiance products across both detectors. In this case the target grid is chosen such that the grid's deviation from the actual λ-θ values of both detector's pixels is minimal at the same time.

4 CONCLUSIONS

It has been shown how PSF non-uniformity and spatial misregistration can affect the radiometry of imaging spectrometry data. Typical numbers as expected for the upcoming APEX system have been examined and led to a variety of noticeable effects. It has been shown that the radiometric accuracy is strongly affected even by moderate PSF variation in the range of 5-20%. Residual errors need to be anticipated in a range of 1-2%. The situation becomes even more critical if high spatial resolution imaging spectroscopy is to be done. Here, residual errors up to 3% could be the result of instable PSF characteristics. Such errors are above the typical critical radiometric stability limit which is at 2%.

If spatial misregistration is evaluated, errors in magnitude of 10% are observed across the whole spectral range, which definitively needs to be corrected by interpolation methods. The correction of misregistration effects seems to be feasible to a certain degree but does not lead to a perfect solution. Low SNR of a sensor severely inhibits correction of PSF and misregistration effects, leaving residual errors in a range of 3%, while a quasi-perfect sensor may be corrected down to an acceptable 1% level. Hence, a residual error in the range of 1-2% is expected even after interpolation, which has to be treated as a radiometric effect due to spatial misregistration.

Given these results, special efforts have to be taken in the APEX PAF software to deal with the depicted anticipated problems in data quality. Sophisticated interpolation routines need to be analyzed and developed in future development to improve the spatial consistency of the data. Moreover, a data model has to be defined which takes track of all interpolation steps to ensure the calibration accuracy of the system.

5 ACKNOWLEDGEMENTS

This work has been supported by the ESA/ESTEC contract 14906/00/NL/DC. NASA/JPL and the AVIRIS team are thanked for providing the AVIRIS data.

6 REFERENCES

Berk, A., L.S. Bernstein, G.P. Anderson, P.K. Acharya, D.C. Robertson, J.H. Chetwynd and S.M. Adler-Golden, 1998: MODTRAN Cloud and Multiple Scattering Upgrades with Application to AVIRIS, *Remote Sens. Environ.* 65:367-37.

Bojinski S., Schaepman M., Schläpfer D. and Itten K., 2003: SPECCHIO: a spectrum database for remote sensing applications. *Computers & Geosciences*, 29:27-38.

Green R.O., Eastwood M.L., Sarture C.M., Chrien T.G., Aronsson M., Chippendale B.J., Faust J.A., Pavri B.E., Chovit C.J., Solis M., Olah M.R. and Williams O., 1998: Imaging Spectroscopy and the Airborne Visible/Infrared Imaging Spectrometer (AVIRIS). *Remote Sens. Environ.*, 65: 227-248.

Itten K.I., Schaepman M., De Vos L., Hermans L., Schlaepfer H. and Droz F., 1997: APEX-Airborne Prism Experiment a New Concept for an Airborne Imaging Spectrometer, Proceedings of the Third International Airborne Remote Sensing Conference and Exhibition. ERIM International Inc., Copenhagen (DK), Vol. I, pp. 181-188.

Kaiser J.W., Schläpfer D., Brazile J., Strobl P., Schaepman M.E. and Itten K.I., 2003: Assimilation of Heterogeneous Calibration Measurements for the APEX Spectrometer, International Symposium on Remote Sensing. *Sensors, Systems, and Next Generation Satellites VII*. SPIE, Barcelona, Vol. 5234, pp. 211-220.

Mouroulis P., Green R.O. and Chrien T.G., 2000: Design of pushbroom imaging spectrometers for optimum recovery of spectroscopic and spatial information. *Applied Optics,* 39(13): 2210-2220.

Schaepman M.E., Itten K.I., Schläpfer D., Kaiser J.W., Brazile J., Debruyn W., Neukom A., Feusi H., Adolph P., Moser R., Schilliger T., De Vos L., Brandt G., Kohler P., Meng M., Piesbergen J., Strobl P., Gavira J., Ulbrich G. and Meynart R., 2003: APEX: Current Status of the Airborne Dispersive Pushbroom Imaging Spectrometer. R. Meynart (Editor), International Symposium on Remote Sensing. *Sensors, Systems, and Next Generation Satellites VII*. SPIE, Barcelona, Vol. 5234, pp. 202-210.

Schläpfer D., Schaepman M., and Strobl P., 2001: Impact of Spatial Resampling Methods on the Radiometric Accuracy of Airborne Imaging Spectrometer Data. 5th Int. Airb. R. S. Conf. and Exh., VERIDIAN, San Francisco & Miami, CD-ROM, pp.8.

Schläpfer D. and Schaepman M., 2002: Modeling the noise equivalent radiance requirements of imaging spectrometers based on scientific applications. *Applied Optics*, 41(27): 5691-5701.

Schläpfer D., Kaiser J.W., Brazile J., Schaepman M.E. and Itten K.I., 2003: Calibration concept for potential optical aberrations of the APEX pushbroom imaging spectrometer, International Symposium on Remote Sensing. *Sensors, Systems, and Next Generation Satellites VII*. SPIE, Barcelona, Vol. 5234, pp. 221-231.

Schowengerdt R.A., 1997: *Remote Sensing: Models and Methods for Image Processing*. Academic Press, 2nd Ed., pp. 522.